# Investigation of p-GaAs/n-$Cd_{1-x}Zn_xS_{1-y}Te_y$/$Cd_{1-x}Zn_xO$ heterojunctions deposited by electrochemical deposition

H. M. MAMEDOV*, V. U. MAMEDOV, V. J. MAMEDOVA, KH. M. AHMADOVA
*Department of Physical Electronics, Faculty of Physics, Baku State University, 370148, Z.Khalilov str., 23, Baku, Azerbaijan*

p-GaAs/n-$Cd_{1-x}Zn_xS_{1-y}Te_y$ anisotype heterojunction without and with $Cd_{1-x}Zn_xO$ oxide films have been fabricated by preparing of n-type $Cd_{1-x}Zn_xS_{1-y}Te_y$ thin films onto the p-GaAs single crystal wafers using an electrochemical deposition method. Cadmium sulfate, zinc sulfate, sodium thiosulfate and tellurium oxide used as a cadmium, zinc, sulfur and tellurium ion in solution, respectively. The voltammetric behavior of the $Cd_{1-x}Zn_xS_{1-y}Te_y$ thin films on GaAs substrate from aqueous solutions was studied. Film's studies were carried out using UV-Vis spectrophotometry, X-ray diffraction (XRD), X-ray fluorescence (XRF) and atomic force microscopy (AFM). The electrical characterization of p-GaAs/n-$Cd_{1-x}Zn_xS_{1-y}Te_y$ heterojunction was performed using current-voltage (*J-V*) and capacitance-voltage (*C-V*) measurements. It is established that heat treatment (HT) at 350-390$^0$C during 8-14 min in argon atmosphere reduces the concentration of defects, results in formation of heterojunctions and minimum values of non-ideality factor of *J-V* characteristics. Under AM1.5 conditions the open-circuit voltage, short-circuit current, fill factor and efficiency of our best cells with $Cd_{1-x}Zn_xO$ films, were $V_{oc}$ = 584 mV, $J_{sc}$ = 14.54 mA/cm$^2$, FF = 0.6 and $\eta$ = 6.7 %, respectively.

(Received April 26, 2013; accepted January 21, 2015)

*Keywords:* Electrochemical deposition, Thin film, Heterojunctions, Heat treatment

## 1. Introduction

Thin films of Cd and Zn chalcogenides are of considerable interest owing to their use in semiconductor device technology and solar cells [1-5]. In photovoltaic system, the replacement of CdS with the higher band-gap $Cd_{1-x}Zn_xS$, $Cd_{1-x}Zn_xS_{1-y}Se_y$ and $Cd_{1-x}Zn_xS_{1-y}Te_y$ (CZSTE) has led to a decrease in window absorption losses and has resulted in an increase in the short-circuit current. The $A^2B^6$ quaternary semiconductors seem to be useful materials photosensitive in the visible and ultraviolet wavelength regions [6-9]. However, single crystals of GaAs are well studied materials; therefore their use at manufacturing of heterojunctions p-GaAs/CZSTE will be good way of deep studying of physical properties of films CZSTE. With a lattice constant of 5.6676 Å, ZnSe epitaxial layers are commonly grown on GaAs substrates having a lattice constant of 5.6535 Å. However, the slight lattice mismatch (i.e., 0.27% at room temperature) between ZnSe and GaAs will still generate a huge amount of defects in ZnSe/GaAs heterojunctions interface [10-11]. The defects generated at the ZnSe/GaAs interface will significantly reduce the efficiency of the ZnSe-based solar cells. One possible way to solve this problem is to use quaternary $Zn_xCd_{1-x}Te_yS_{1-y}$ (x=0.7-0.75; y=0.2) as the material of solar cells. By carefully controlling the composition ratio between cadmium, zinc, sulfur and tellurium, one should be able to grow x=0.7-0.75; y=0.2 CZSTE films perfectly matched to the GaAs substrate.

Traditional way of fabricating solar cells on the basis of Cd and Zn chalcogenides is to grow window materials using thermal evaporation, magnetron sputtering and MOVPE. Electrochemical deposition is a perspective competitor in thin film preparation because of several advantages such as the possibility for large-scale production, minimum waste of components and easy monitoring of the deposition process. This technique is generally less expensive than those prepared by the capital-intensive physical methods.

In the present work, anisotype heterojunction of p-GaAs/n-CZSTE was fabricated by depositing of CZSTE thin films as a window using the electrochemical deposition method onto the p-GaAs single crystals.

## 2. Experimental

Electrodeposition of the CZSTE films (with thickness of 350-400 nm) onto the p-GaAs substrates was carried out at temperature of 80°C from aqueous solution containing cadmium ($CdSO_4$), zinc ($ZnSO_4$), sodium ($Na_2S_2O_3$) and tellurium ($TeO_2$ or $Na_2Te_2O_3$) salts. The thickness and resistivity of the monocrystalline p-GaAs substrates were 0.4 mm and $\rho$ = 0.2-0.23 Ω·cm, respectively. Before the deposition process, the surfaces of GaAs substrates were etched in an aqueous solution of hydrochloric acid (HCl) and KOH-$KNO_3$ (1:3) composition for 3 min. After etching the GaAs wafers were washed for 2 min in pure alcohol and distilled water, which it was maintained at high temperatures (≥ 300°C).

In order to fabricate the heterojunctions, an ohmic In electrode, in reticulose form was evaporated on the $Cd_{0.25}Zn_{0.75}S_{0.8}Te_{0.2}$ films with an area of ~0.82-1 cm$^2$. An ohmic contact was performed on the side of GaAs wafers by evaporating an Al electrode. Thermal annealing of

heterojunctions in argon atmosphere was carried out in thermogravimeter TQA-50.

Photoelectric properties of heterojunctions p-GaAs/n-CZSTE were investigated without and with $Cd_{1-x}Zn_xO$ oxide layers. Thin films of $Cd_{1-x}Zn_xO$ with different compositions (x=0.6; 0.7 and 0.8) also were deposited by electrochemical deposition through $Zn(NO_3)_2$ + $Cd(NO_3)_2$ aqueous solutions at room temperature. The distance between the electrodes was about 0.5 cm. Electrodeposition was carried out at the current density of 4 mA/cm$^2$. The pH was adjusted to 5-7, and the deposition time was 1.5-2 h. The thickness of $Cd_{1-x}Zn_xO$ were 170-230 nm.

### 3. Results and discussion

Cyclic voltammetry was used to monitor the electrochemical reactions in solutions of $CdSO_4$, $ZnSO_4$, $Na_2S_2O_3$ and $TeO_2$, then in their combined solution of the same concentration and pH. The cyclic voltammogram was scanned in the potential range 1.2 V to –1.2 V versus graphite (or Ag/AgCl) electrodes. In the case of $CdSO_4$ solution, the current rise started at –0.15 V, followed by large reduction wave at –0.9 V. This response was associated with Cd reduction on GaAs substrate. The deposition reaction was reconfirmed by the reverse scan. The two stripping peaks at positive potential limits, 0.6-0.9 V indicated the oxidation of the cadmium compound. Cyclic voltammogram for $ZnSO_4$ showed a reduction potential starting at about –0.83V. This was due to the reduction process of Zn onto the working electrode. The reduction peak increased towards the more-negative region where hydrogen evolution also occurred.

The forward scan of $Na_2S_2O_3$ and $Na_2Se_2O_3$ solutions shows the cathodic current to start flowing at about –0.2-0.4V. The shoulder at –0.75-0.8V might be associated with the reduction of $Na_2S_2O_3$ and $Na_2Se_2O_3$ ions. Cyclic voltammogram for mixture of $CdCl_2$, $ZnCl_2$, $Na_2S_2O_3$ and $Na_2Se_2O_3$ salts, shows that wave around –0.62-0.88V corresponded to the formation of $Cd_{0.25}Zn_{0.75}S_{0.8}Te_{0.2}$ layers.

Table 1 shows the deposition potential for different composition of CZSTE films.

*Table 1. Mole fraction of salts, deposition current and potential for the CZSTE films*

| Composition of $Cd_{1-x}Zn_xS_{1-y}Te_y$ films | | Mole fraction of salts | | | | Deposition current and potential | |
|---|---|---|---|---|---|---|---|
| x | y | $CdSO_4$ (M) | $ZnSO_4$ (M) | $Na_2S_2O_3$ (M) | $TeO_2$ (M) | J, mA/cm$^2$ | $U_c$ (V) |
| 0.1 | 0.1 | 0.92 | 0.12 | 0.9 | 0.12 | 10-11 | 0.78 |
| 0.1 | 0.2 | 0.9 | 0.1 | 0.83 | 0.15 | 14-17 | 0.65 |
| 0.1 | 0.3 | 0.91 | 0.13 | 0.71 | 0.28 | 18-21 | 0.61 |
| 0.1 | 0.4 | 0.93 | 0.12 | 0.58 | 0.4 | 20-22 | 0.58 |
| 0.1 | 0.5 | 0.92 | 0.1 | 0.52 | 0.5 | 21-24 | 0.52 |
| 0.2 | 0.1 | 0.81 | 0.21 | 0.91 | 0.1 | 9-11 | 0.83 |
| 0.25 | 0.1 | 0.82 | 0.23 | 0.9 | 0.1 | 8-11 | 0.84 |
| 0.3 | 0.2 | 0.7 | 0.29 | 0.8 | 0.18 | 10-11 | 0.8 |
| 0.4 | 0.2 | 0.58 | 0.42 | 0.8 | 0.18 | 9-11 | 0.83 |
| 0.5 | 0.5 | 0.5 | 0.49 | 0.5 | 0.5 | 12-13 | 0.81 |
| 0.6 | 0.5 | 0.4 | 0.6 | 0.5 | 0.5 | 11-12 | 0.82 |
| 0.7 | 0.2 | 0.31 | 0.7 | 0.81 | 0.19 | 10-11 | 0.83 |
| 0.75 | 0.2 | 0.23 | 0.77 | 0.8 | 0.2 | 9-11 | 0.84 |
| 0.8 | 0.2 | 0.2 | 0.82 | 0.8 | 0.2 | 8-10 | 0.86 |
| 0.9 | 0.2 | 0.11 | 0.89 | 0.81 | 0.21 | 8-9 | 0.9 |
| 0.9 | 0.1 | 0.1 | 0.9 | 0.91 | 0.1 | 7-9 | 0.94 |
| 0.8 | 0.1 | 0.2 | 0.8 | 0.9 | 0.1 | 10-12 | 0.85 |
| 0 | 1 | | 0.5 | | 0.5 | 27-33 | 0.31 |
| 1 | 1 | | 0.5 | | 0.5 | 22-27 | 0.45 |

In order to achieve a more direct insight into the surface structural features of the films, AFM imaging had been performed. AFM images of thin films $Cd_{0.25}Zn_{0.75}S_{0.8}Te_{0.2}$ deposited at various deposition potentials are shown in Figure 1 in an area of 10μm x 10μm. As seen from the images the films deposited at -0.6 V revealed an incomplete coverage of the substrate surface and showed that grains are not distributed uniformly over the substrate.

The films deposited at - 0.84 V proved that its surface was compact, uniform, and smooth. The grain sizes were in the range from 0.01 to 0.2 μm. The films surface is not uniform for cathodic potentials more -0.9 V. The size of the grains was different from each other, indicating irregular growth rate of the grains.

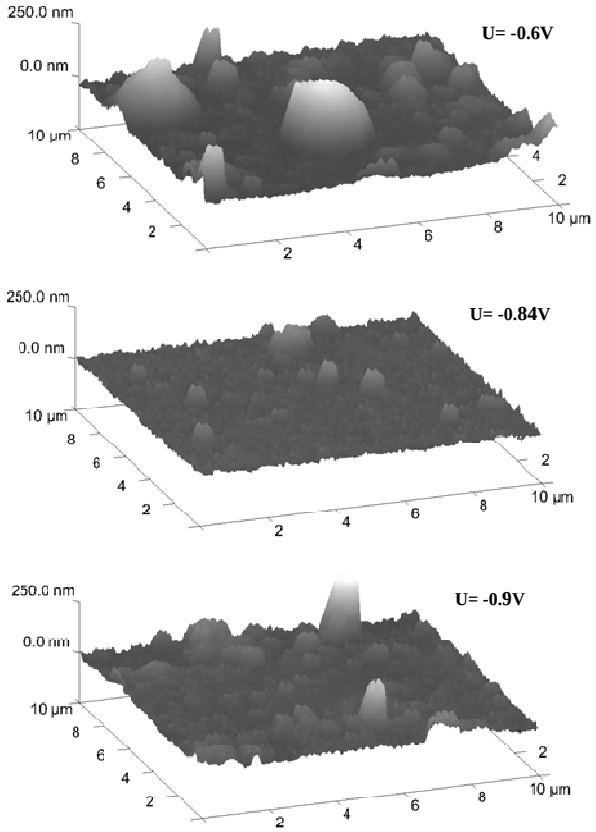


*Fig. 1. Atomic force microscopy images of $Cd_{0.25}Zn_{0.75}S_{0.8}Te_{0.2}$ thin films deposited at different deposition potential*

The stoichiometry of the CZSTE films was investigated using XRF in order to correlate the material and atomic percentages of individual elements. Figure 2 shows the XRF analysis for $Cd_{0.25}Zn_{0.75}S_{0.8}Te_{0.2}$ thin films deposited at different cathodic potential. As seen from the figure at voltage of 0.84 V, the material becomes stoichiometric, reaching 25 at% for Cd and 20 at% for Te.

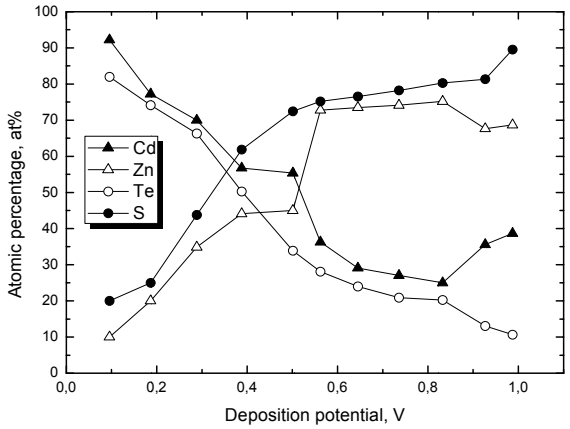


*Fig. 2. XRF analyses showing the atomic percentages of Cd, Zn, S and Te for the $Cd_{0.25}Zn_{0.75}S_{0.8}Te_{0.2}$ thin films deposited at different deposition potentials*

Fig. 3 shows the XRD patterns of $Cd_{0.25}Zn_{0.75}S_{0.8}Te_{0.2}$ thin films. All the as deposited CZTE thin films are amorphous. It can be obviously seen from figure that as the temperature increases from 100 to 390$^0$C for 14 min, the intensities of the peaks increase, implying an improvement in crystallinity. The high intensity of the substrate peak (GaAs) compared to the compound peak shows that the film thickness is low due to insufficient deposition time. The obtained d-spacing values corresponds well the standard Joint Committee on Powder Diffraction Standard data. The XRD results obtained indicated that the films were polycrystalline in nature. The films deposited for this period was smooth and adhered well towards the substrate. However when the deposition time was increased to $\tau \geq 20$ minutes, the presence of additional peaks, which does not correspond to CdS-ZnTe system, was obtained. This is phenomenon may occur due to co-deposition of elemental materials due to long immersion time in the deposition bath.

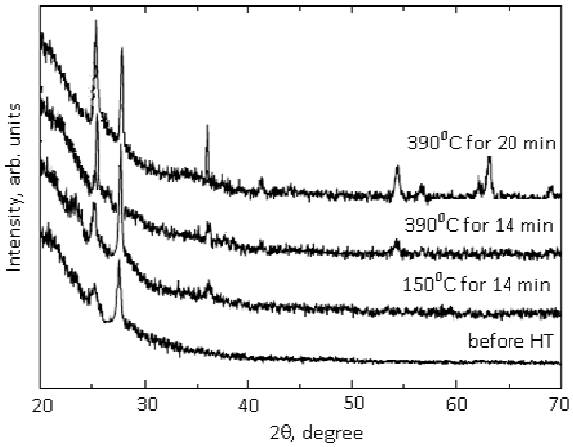


*Fig. 3. X-ray diffractograms of $Cd_{0.25}Zn_{0.75}S_{0.8}Te_{0.2}$ thin films before and after HT*

The wavelength dependence of the optical transmittance of the CZSTE films (after the HT in argon atmosphere at 390$^0$C for 14 min) with different contents of Zn and Te are shown in Fig. 4. As seen from the figures, the transmittance of the films increased from 74% to 78% above the fundamental absorption edge with increase of Zn and S content, which indicates better crystallinity of the films. Also, the fundamental absorption edge of the films shifted towards the shorter wavelength side with the increase of Zn-concentration and decrease of Te-concentration. From the absorbance data, the absorption coefficient (α) at frequency of radiation calculated from the relationship $\alpha(\nu) = \dfrac{\ln(1/T)}{d}$. Where *d*- is the thickness of the films and *T*- is the optical transmittance.

The optical absorption edge was analyzed by the following relationship:

$$\alpha(\nu) = \frac{A\left(h\nu - E_g\right)^n}{h\nu} \quad (1)$$

Where $A$ is a constant, $n$ values are 1/2 and 2 for direct and indirect transitions, respectively. The curves of $ln(\alpha h\nu)$ versus $ln(h\nu\text{-}E_g)$ were plotted using the $E_g$ value to determine the value of $n$ and it was found to about 1/2 from the slope of this curves. It is established that films of CZSTE are materials with direct band gap.

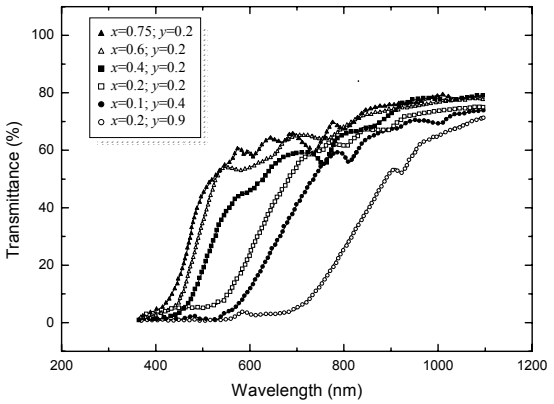


*Fig. 4. Wavelength dependence of optical transmittance for CZSTE films after the H T in argon atmosphere at 390$^0$C for 14 min*

A plot of $(\alpha h\nu)^2$ versus $h\nu$ for different compositions of CZSTE films are shown in Figure 5. The bandgap of the CZSTE films were determined from extrapolation of the straight line section of the $(\alpha h\nu)^2$ versus $h\nu$ curves. The linear nature of the plots at the absorption edge confirmed that CZSTE films are semiconductors with a direct bandgap. This reveals that uniform and device quality films can be prepared by electrodeposition technique. The constant $A$ were calculated from the linear region of the plots $(\alpha h\nu)^2$ versus $h\nu$ and is listed in Table 2.

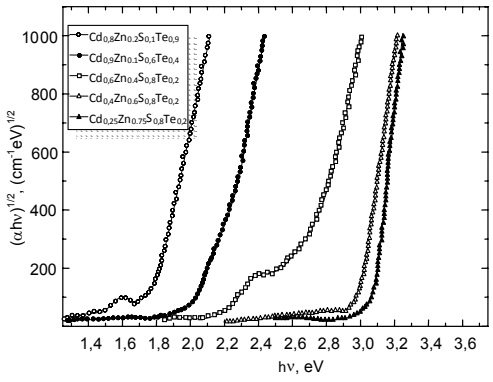


*Fig. 5. Plots of $(\alpha \cdot h\nu)^{1/2}$ versus photon energy for CZSTE films with different compositions*

*Table 2*

| Composition of CZSTE films | | $E_g$, (eV) Direct energy bandgap | A, ($cm^{-1}\cdot eV^{1/2}$)×$10^{10}$ |
|---|---|---|---|
| *x* | *y* | | |
| 0.1 | 0.4 | 2.12 | 3.1 |
| 0.2 | 0.9 | 1.77 | 1.7 |
| 0.4 | 0.2 | 2.65 | 2.3 |
| 0.6 | 0.2 | 2.9 | 2.9 |
| 0.75 | 0.2 | 3.1 | 3.6 |

The dark current-voltage (*J-V*) curves of the heterojunctions were measured in the direct and reverse current modes. The experimental *J-V* curves, measured at 300 K, for as-deposited p-GaAs/n-$Cd_{1-x}Zn_xS_{1-y}Te_y$ heterojunction using various values of $x$ and $y$ are illustrated in Fig. 6. These curves were definitely of the diode type, with the forward direction corresponding to the positive potential on p-GaAs. Thus, according to this figure, the rectification in the as-deposited junctions on the basis of CZSTE films with $x$=0.75 and $y$=0.2 (which is good lattice matched to GaAs layers) reaches value of 700 at voltage $U$ = 1.0 V, and decreases when zinc concentration $x$ increases. The low value of the rectification coefficient is caused by the high series resistance within the heterostructure.

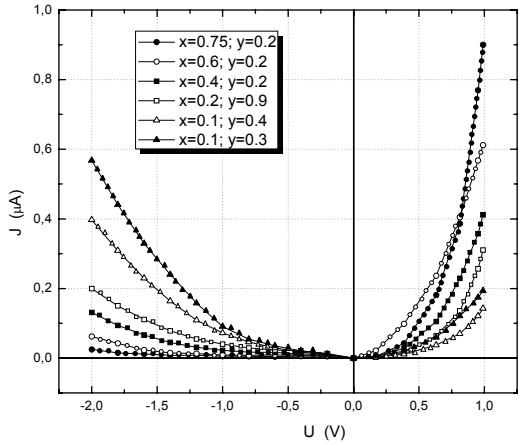


*Fig. 6. Dark J-V curves for as-deposited p-GaAs/n-$Cd_{1-x}Zn_xS_{1-y}Te_y$ heterojunction*

Dark *J-V* curves in a *lnJ = f(U)* plot for p-GaAs/n-$Cd_{1-x}Zn_xS_{1-y}Te_y$ -as deposited heterojunctions are shown in Figure 7. Plotting the natural log of the current density versus the applied voltage, we are able to identify a characteristic thermally activated recombination region up to 0.63 V. Usually, such dependencies are described by the expression

$$J = J_0[\exp(\frac{eV}{AkT}) - 1] \quad (2)$$

Here, $J_s$ is the saturation current density, $V$ is the applied voltage, $e$ is the electron charge, $A$ is the ideality factor, $k$ is the Boltzmann constant, and $T$ is the temperature.

Further increase of the forward bias magnitude (U>0.65 V) results in the less steep dependence of *J(V)* and its pronounced deviation from the curve calculated according to the formula (2), which can be the consequence of the changes of carrier transport mechanism. The most possible case to be considered is tunneling recombination. The ideality factor is determined under a forward bias, and in the as-deposited heterojunctions, it is normally found to range from 1.6 to 2.7 for the different $x$ and $y$. As seen from the figure the value of ideality factor for the heterojunctions p-GaAs/n-$Cd_{0.25}Zn_{0.75}S_{0.8}Te_{0.2}$ are minimum.

It is found that the mechanism of current passage through the heterojunctions essentially changes with increasing HT temperature from 0 to 390°C (for 14 min): tunnel currents sharply decrease, which shows the reduction of defects and decreasing of the series resistance (Figure 8). In the annealing in argon atmosphere at 390°C for 14 min, the ideality factor values were approximately 1.4 for the heterojunctions with $x$=0.75 and $y$=0.2. It is significant to note that the best rectification for the annealed p-GaAs/n-$Cd_{0.25}Zn_{0.75}S_{0.8}Te_{0.2}$ heterojunctions was obtained at about $k$ = 3000, which is attributable to the optimal annealing conditions and the lattice mismatch between the solid solution and GaAs.

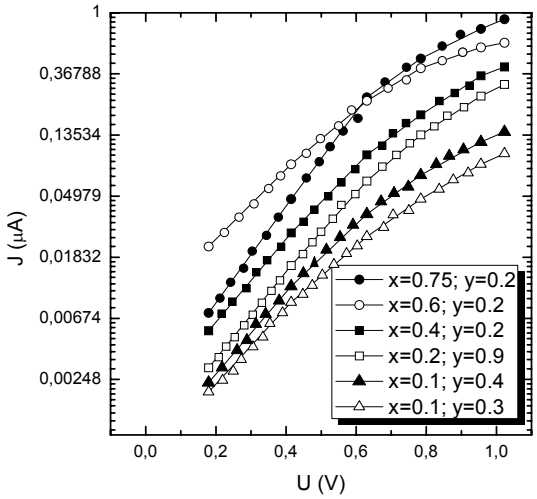


*Fig. 7. Semilogarithmic plot of forward bias of J-V curves for p-GaAs/n-$Cd_{1-x}Zn_xS_{1-y}Se_y$ –as-deposited heterojunctions at different x and y.*

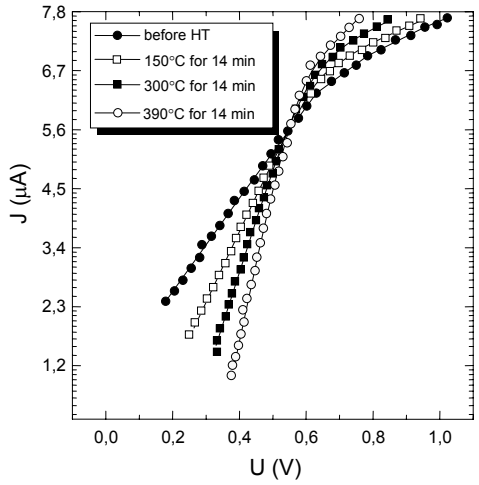


*Fig. 8. Semilogarithmic plot of forward bias of J-V curves for p- GaAs/n- $Cd_{0.25}Zn_{0.75}S_{0.8}Te_{0.2}$ heterojunctions at different regimes of HT.*

Fig. 9 shows the capacitance versus voltage measurement results ($1/C^2$-$V$) for the heterojunctions p-GaAs/n-$Cd_{0.25}Zn_{0.75}S_{0.8}Te_{0.2}$ annealed in argon atmosphere at 390°C for 14 min. This plot shows a linear relationship with bias voltage and indicates that the junction is abrupt. Also built–in potential ($V_{bi}$ = 0.61 V) were calculated by extrapolating ($1/C^2$-$V$) plot to (($1/C^2$)=0).

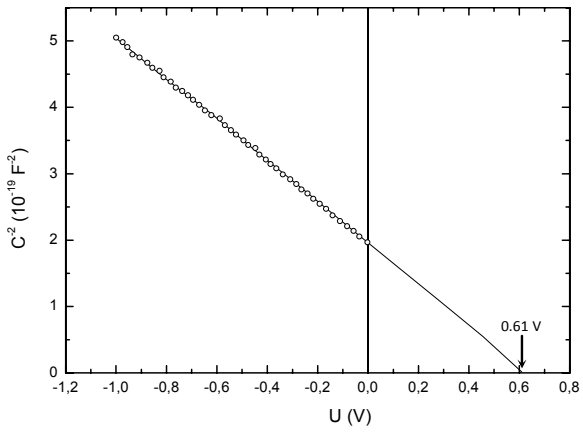


*Fig. 9. Capacitance-voltage dependences for p-GaAs/n-$Cd_{0.25}Zn_{0.75}S_{0.8}Te_{0.2}$ heterojunctions after the HT at 390°C for 14 min*

We also studied the effect of HT on the photoelectric properties of these heterojunctions without and with $Cd_{1-x}Zn_xO$ (x=0.6; 0.7 and 0.8) oxide layers (Fig. 10 and 11).

Fig. 10 shows the room temperature photoresponse curves of the p-GaAs/n-$Cd_{0.25}Zn_{0.75}S_{0.8}Te_{0.2}$ heterojunctions without $Cd_{1-x}Zn_xO$ oxide layers before and after HT. There occurs a reconstruction of the photosensitivity spectrum after HT, i.e. the spectrum broadens. As the annealing temperature increased from 0 to 390°C for 14 min, photosensitivity in the $\lambda_m$ = 0.38 – 0.8 μm wavelength region sharply increased. The near infrared photosensitivity falloff for all heterojunctions indicated GaAs absorber band gaps of 1.42 eV. Figure 10 also shows that after subsequently annealing in argon atmosphere for > 14 min at 390°C-400°C the performance of these cells deteriorated. The value of short-circuit-photocurrent varies nonmonotonically with HT duration. Initially, $J_{sc}$ increases with duration, reaches a maximum value and at >14 min, decreases drastically. Under AM1.5 conditions the maximal values of open-circuit voltage, short-circuit current, fill factor and efficiency of our best cell without $Cd_{1-x}Zn_xO$ oxide layers, were $V_{oc}$ = 540 mV, $J_{sc}$ = 11.86 mA/cm$^2$, FF = 0.54 and η = 5.4 %, respectively.

Fig. 11 shows the photosensitivity spectrum of the heat treated at 390°C for 14 min heterojunctions p-GaAs/n-$Cd_{0.25}Zn_{0.75}S_{0.8}Te_{0.2}$ without and with $Cd_{1-x}Zn_xO$ oxide layers. The spectral response curve shows an increase of the short wavelength photosensitivity the solar cells with $Cd_{1-x}Zn_xO$ films. This finally results in that the efficiency of the solar cells coated by $Cd_{1-x}Zn_xO$ are improved by a value of 11 % ($V_{oc}$ = 584 mV, $J_{sc}$ = 14.54 mA/cm$^2$, FF = 0.6 and η = 6.7 %).

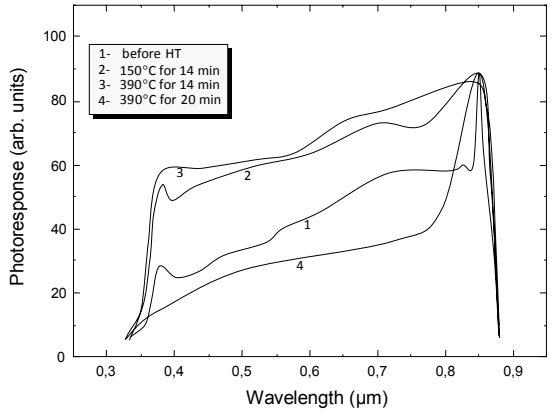


*Fig. 10. Plots of photoresponse against wavelength for p-GaAs/n-$Cd_{0.25}Zn_{0.75}S_{0.8}Te_{0.2}$ heterojunctions before and after HT measured at zero bias.*

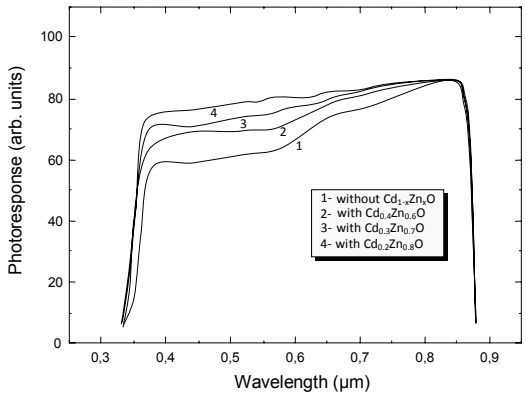


*Fig. 11. Plots of photoresponse against wavelength for p-GaAs/n-$Cd_{0.25}Zn_{0.75}S_{0.8}Te_{0.2}$ heterojunctions with $Cd_{1-x}Zn_xO$ films measured at zero bias.*

## 4. Conclusion

Anisotype heterojunction of p-GaAs/$Cd_{1-x}Zn_xS_{1-y}Te_y$ are fabricated by the electrodeposition method. Their base characteristics were studied depending on the composition of $Cd_{1-x}Zn_xS_{1-y}Te_y$ films, deposition potential and the HT condition. It is established that HT at 390°C for 14 min in argon atmosphere reduces the concentration of defects, results in formation of heterojunctions and minimum values of non-ideality factor of *J-V* characteristics. Heterojunctions with $x$ = 0.75 and $y$ = 0.2 possess a high photosensitivity after the HT in argon at 390°C for 14 min. Under standard 100 mW/cm$^2$ white-light illumination at room temperature, the values of the parameters of our best cell with $Cd_{1-x}Zn_xO$ films were $V_{oc}$ = 584 mV, $J_{sc}$ = 14.54 mA/cm$^2$, FF = 0.6 and η = 6.7 %, respectively.

### Acknowledgment

This work was supported by FP7 NAPEP project № 266 600.

### References

[1] Y. Raviprakash, K. V. Bangera, G. K. Shivakumer, Curr. Appl. Phys. **10**, 193 (2010).
[2] M. C. Baykul and Orhan, Thin Solid Films **518,** 1925 (2010)
[3] A. Sh. Abdinov, H. M. Mamedov, S. I. Amirova, Japanese Journal of Applied Physics, **46,** 7359 (2007).
[4] A. Sh. Abdinov, H. M. Mamedov, S. I. Amirova, Thin Solid Films, **511-512,** 140 (2006).

[5] A. Sh. Abdinov, H. M. Mamedov, G.I. Garibov, N. A. Ragimova, Optoelectron. Adv. Mater. – Rapid Commun., **1,** 480 (2007).
[6] S. Fujii, N. Tasaki, N. Shinomura, S. Kurai, Y. Yamada and T. Taguchi, Journal of Light & Visual Environment, **31,** 61 (2007).
[7] S. J. Chang, H. S. Hsiao, J. Y. Wang, Nanoscale Res Lett, **4**, 1540 (2009).
[8] U. Paliwal, R. K. Kothari, K. B. Joshi, Superlattices and Microstructures, **51,** 635( 2012).
[9] H. M. Mamedov, V. U. Mamedov, Journal of Qafqaz University, **34** 71 (2012).
[10] J. W. Balch, W. W. Anderson, Physics Status Solidi (a), **9,** 567 (2006).
[11] O. Briot, N. Briot , T. Cloitre , R. L. Aulombard, B. Gil, H. Mathieu, Semiconductor Science and Technology, **6,** 695 (2001).

*Corresponding author: mhhuseyng@gmail.com